CI&CEQ
Chemical Industry & Chemical Engineering Quarterly

Available online at
Association of the Chemical Engineers of Serbia AChE
www.ache.org.rs/CICEQ

Chem. Ind. Chem. Eng. Q. 30 (4) 325–333 (2024) CI&CEQ

GOLDEN STEPHA NALLATHAMBI[1]
BHARATHI GOWRI SASI KUMAR[2]
GUVVA SWATHY[3]

[1]Department of Mathematics, R.M.K Engineering College, India
[2]Department of Mathematics, Ethiraj College for Women, India
[3]Mathematics Department, S. A. Engineering College, India

THE MAGNETOHYDRODYNAMIC WILLIAMSON FLUID FLOW ON AN EXTENDING SHEET WITH THERMOPHORESIS AND CHEMICAL REACTION

Article Highlights

- Non-linear system of Partial differential equations
- MATLAB bvp4c solver is used
- Examines velocity, temperature, and concentration distribution of Williamson fluid
- Chemical reaction, thermophores, and magnetic field parameters are analyzed

Abstract

This research investigates the steady, two-dimensional, incompressible flow of a pseudoplastic Williamson fluid subjected to a linearly stretched sheet. The study incorporates the effects of magnetic fields, chemical reactions, and thermophoresis on fluid behavior. By applying boundary layer techniques and similarity transformations, the governing equations are simplified for numerical analysis. The MATLAB bvp4c solver is employed to solve the reduced equations. The obtained results are visually represented and thoroughly discussed to comprehend the model's physical characteristics. The investigation highlights the magnetic field's influence, chemical reaction, and impact of thermophoresis particle deposition on the flow behavior of Williamson fluid over the extended sheet. Moreover, significant roles are found for chemical reactions and thermophoresis parameters in determining the fluid concentration near the boundary layer. It is observed that an increase in the chemical reactions and thermophoresis parameters results in a reduced thickness of the fluid concentration near the boundary layer. Notably, an increase in Schmidt value also diminished the thickness of the fluid concentration close to the boundary layer. The magnetohydrodynamic parameter significantly influences the fluid's velocity and temperature near the surface. It has been noted that an increase in the magnetohydrodynamic parameter decreases the fluid's velocity and increases the temperature near the surface. The impact of skin friction coefficient and Nusselt number and the impact of mass transfer coefficient on Williamson fluid will be discussed. The findings acquired are examined in relation to existing research and the correlation is provided as a table.

Keywords: Williamson fluid, magnetohydrodynamics, chemical reaction, thermophoresis.

SCIENTIFIC PAPER

UDC 544.33.03:66

Pseudoplastic fluids are commonly encountered in various applications and industries, making their boundary layer flow an area of significant research interest. Numerous models have been proposed to characterize the behaviour of pseudoplastic fluids; however, the Williamson fluid model has received relatively limited attention. In 1929, Williamson [1] conducted pioneering research on the flow of pseudoplastic materials. He suggested a model equation to explain pseudoplastic fluid flow and

Correspondence: G.S. Nallathambi, Department of Mathematics, R.M.K Engineering College, India.
E-mail: ngs.sh@rmkec.ac.in
Paper received: 28 September, 2023
Paper revised: 20 January, 2024
Paper accepted: 24 February, 2024

https://doi.org/10.2298/CICEQ230928005N

validated the conclusions through empirical data analysis. Despite its potential significance, the Williamson fluid model remains an underexplored aspect of pseudoplastic fluid dynamics.

In the realm of boundary layer flow, pioneering research was conducted by Sakiadis [2] on a continuously stretched surface, where he created the fundamental equations for boundary layers in two dimensions. Subsequently, Tou *et al.* [3] examined how transfer processes affect boundary layer flow on a stretching surface in depth. Erickson *et al.* [4] expanded the study to include the impacts of mass transfer, taking into account both injection and suction.

Nadeem *et al.* [5] explored the intriguing Williamson fluid behavior on a stretched sheet, revealing that as the Williamson parameter increased, velocity profiles and skin friction coefficient deteriorated. Continuing this investigation, Hayat *et al.* [6] delved into the complexities of Williamson fluid flow across a stretched surface with a magnetic field, heat radiation, and an electric field. Their findings indicated that greater values of the Williamson parameter resulted in a reduction in the wall shear stress.

Shawky *et al.* [7] brought a new perspective by analyzing the movement of a non-Newtonian fluid under the influence of a magnetic field over an extended porous sheet. They observed that when the Williamson and porosity parameters increased, the rate of heat transfer to the expanded surface significantly increased. These studies collectively shed light on the intricate dynamics of pseudoplastic fluids like Williamson fluid in various boundary layer flow scenarios, offering valuable insights for practical applications in industry and engineering. In the realm of Williamson fluid dynamics, Hussain [8] conducted a comprehensive study on the influence of nanoparticles on Williamson fluid flow over a stretching sheet. The findings revealed that various physical parameters significantly impacted heat transfer near the wall, while their effects were nearly negligible farther away from the wall.

Further exploring the characteristics of Williamson nanofluids, Nadeem and Hussain [9] investigated Williamson nanofluid magnetohydrodynamic (MHD) flow over a heated surface. Notably, they discovered that the Williamson fluid's conductivity was lower than that of Williamson nanofluid., emphasizing the importance of considering nanoparticle additives for enhanced thermal performance. Delving into the complexities of Williamson nanofluids' boundary layer stream, Kebede *et al.* [10] analyzed its stability and revealed that the velocity profile decreased as a function of various parameters, including Williamson, porosity, unsteadiness, and magnetic field parameters. These studies collectively provide valuable insights into the behavior of Williamson nanofluids, paving the way for potential applications in heat transfer and fluid dynamics research.

Numerous researchers have contributed to the understanding of the progress of boundary layers on surfaces that are linearly stretched [11–13]. Kumaran and Ramanaiah [14] investigated viscous fluid flow over a stretching surface with quadratic stretching, obtaining closed-form solutions. Ali [15] examined the thermal boundary layer's response to temperature changes and power law stretching. Elbashbeshy[16] talked about how viscous fluid flows and transfers heat under exponential stretching conditions.

By including viscous dissipation and elastic deformation, Sanjayanand and Khan [17] expanded the study to consider heat and mass transmission of viscoelastic fluid. A numerical solution for the heat and mass transfer of a viscous fluid over an exponentially extending surface was created by Magyari and Keller [18]. In their examination of the thermal radiation impacts of Jeffery fluid over an exponentially extending surface, Nadeem *et al.* [19] compared the numerical and homotopy analysis method (HAM) results. More recently, Nadeem and Lee [20] investigated the impact of nanoparticles on the exponentially stretched boundary layer flow of viscous fluid.

Numerous processes also depend on the analysis of integrated heat and mass transfer associated with chemical reactions including radioactive waste geo-repositories, packed bed chemical reactors, and heat exchangers used to cool electronic circuits. Chemical concentration is examined by numerous scholars [21–23].

The MHD flow over a stretching sheet has abundant industrial and manufacturing applications, which include polymer extrusion, continuous casting of metals, petroleum industries, and electrical power generators. Due to its large-scale applications, many researchers attempted to study and analyze the solutions of differential equations describing boundary layer and MHD fluid flow problems along a stretching sheet. Mohammed Ismail *et al.*[24] addressed the effect of thermal radiation on MHD hybrid nanofluid flow over a stretching cylinder immersed in a porous medium and discussed the various physical properties. They further extended the work in the investigation of numerically solving the heat transfer enhancement due to the radiative magnetohydrodynamics flow of a hybrid nanofluid past a porous stretching cylinder under the influence of variable viscosity as well as suction [25]. Subsequently, SM Ismail *et al.* [26] have analyzed the MHD flow of an aqueous ethylene glycol nanofluid past

a two-way exponentially extending lamina where appropriate transformation is used, thereby the temperature and velocity sketches of copper alumina in aqueous glycol nanofluid for current physical stratum are obtained.

The thermophoresis phenomenon is essential in many practical applications including the removal of small particles from gas streams, aerosol technology, deposition of silicon thin films, and radioactive particle deposition in nuclear reactor safety simulations. Several studies discussed the impact of thermophoresis particle deposition in the literature [27–28].

Williamson fluid over a continuously moving surface is often encountered in engineering such as polymer processing industries, paint and coatings manufacturing, food processing, inkjet printing, wastewater treatment, etc. Understanding the rheological properties of Williamson fluid is crucial in these engineering applications to optimize processes, ensure proper functionality, and achieve desired product characteristics.

In the current work, we focus on the mass and heat transfer analysis of Williamson fluid over a linearly stretching sheet, leveraging the Williamson fluid model, while considering the influence of a magnetic field, chemical reaction, and thermophoresis. By employing suitable similarity transformations, we simplify the governing boundary layer equations. The resulting equations are solved using numerical methods, and the outcomes are presented through graphs, offering valuable insights into the behavior of the Williamson fluid under linearly stretching conditions.

PROBLEM FORMULATION

Consider the Williamson fluid model, which is incompressible, steady, and capable of mass transfer while flowing over a linearly stretched sheet in two dimensions in the presence of the following physical properties: chemical reaction, thermophoresis, MHD, viscous dissipation.

The equations represent a comprehensive system that describes the conservation of mass, momentum, energy, and concentration for the Williamson fluid flow over the linearly stretched sheet, considering the effects of chemical reaction, thermophoresis, and magneto-hydrodynamics are [6,29].

$$\frac{\partial u}{\partial x}+\frac{\partial u}{\partial y}=0 \tag{1}$$

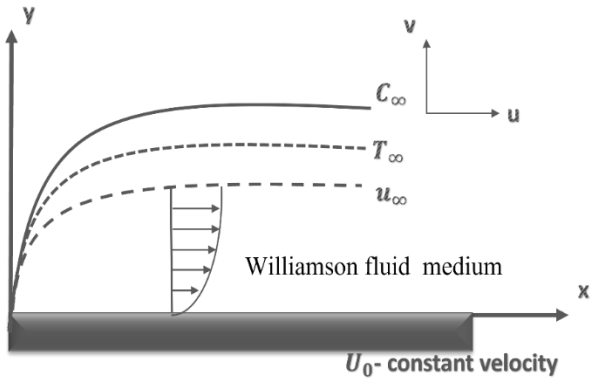

Figure 1. Schematic diagram.

$$u\frac{\partial u}{\partial x}+v\frac{\partial u}{\partial y}=v\frac{\partial^2 u}{\partial y^2}+\sqrt{2}v\Gamma\frac{\partial u}{\partial y}\frac{\partial^2 u}{\partial y^2}-\left(\frac{\sigma B^2(x)}{\rho c_p}\right)u \tag{2}$$

$$u\frac{\partial T}{\partial x}+v\frac{\partial T}{\partial y}=\frac{k}{\rho c_p}\left(\frac{\partial^2 T}{\partial y^2}\right)+\frac{v}{c_p}\left(\frac{\partial u}{\partial y}\right)^2-\left(\frac{\sigma B^2(x)}{\rho c_p}\right)u^2 \tag{3}$$

$$u\frac{\partial C}{\partial x}+v\frac{\partial C}{\partial y}=D\frac{\partial^2 C}{\partial y^2}-R_C(C-C_\infty)-\frac{\partial}{\partial y}\left(V_T(C-C_\infty)\right) \tag{4}$$

where the magnetic conduction is $B(x)=\frac{B_0}{\sqrt{2x}}$.

Because of the magnetic conduction, Eqs. (2) and (3) becomes:

$$u\frac{\partial u}{\partial x}+v\frac{\partial u}{\partial y}=v\frac{\partial^2 u}{\partial y^2}+\sqrt{2}v\Gamma\frac{\partial u}{\partial y}\frac{\partial^2 u}{\partial y^2}-\left(\frac{\sigma B_0^2}{\rho 2xc_p}\right)u \tag{5}$$

$$u\frac{\partial T}{\partial x}+v\frac{\partial T}{\partial y}=\frac{k}{\rho c_p}\left(\frac{\partial^2 T}{\partial y^2}\right)+\frac{v}{c_p}\left(\frac{\partial u}{\partial y}\right)^2-\left(\frac{\sigma B_0^2}{\rho 2xc_p}\right)u^2 \tag{6}$$

Subject to the boundary conditions:

$$\begin{aligned}&u=U_0, T=T_W, C=C_W \ \ at\ \ y=0\\&u=0, T=T_\infty, C=C_\infty \ at\ y\to\infty\end{aligned} \tag{7}$$

where the velocities along the x and y axes are denoted by u and v respectively. v is the kinematic velocity.

By using the following similarity transformations [6,27]:

$$\eta=y\sqrt{\frac{U_0}{2\gamma x}},\ \psi=\sqrt{2\gamma U_0 x}f(\eta),\ \psi-\ \text{stream function}$$

$$u=\frac{\partial\psi}{\partial y}, v=-\frac{\partial\psi}{\partial x}$$

$$\begin{aligned}&u=U_0 f'(\eta), v=-\frac{1}{2}\sqrt{\frac{2U_0\gamma}{x}}f+\frac{1}{2}\frac{U_0 y}{x}f'\\&T=(T_w-T_\infty)\theta(\eta)+T_\infty\\&C=(C_w-C_\infty)\varphi(\eta)+C_\infty\end{aligned} \tag{8}$$

Substituting Eq. (8) in Eq. (1), which is satisfied identically. After applying the above similarity

transformations, Equations (2–4) becomes:

$$f'''+\lambda f''f'''+ff''-Mf'=0 \quad (9)$$

$$\theta''+P_r\theta'f+P_rE_cf''+\mathrm{MP}_rE_cf'^2=0 \quad (10)$$

$$\varphi''+\mathrm{Sc}\left(f\varphi'+\mathrm{R}\varphi-\mathrm{T}_V\theta''\right)=0 \quad (11)$$

corresponding boundary conditions are:

$$\begin{aligned} &f'(0)=1,\theta(0)=1,\phi'(0)=1\\ &f'(\infty)=0,\theta(\infty)=0,\phi'(\infty)=0 \end{aligned} \quad (12)$$

where,

Magnetic Parameter $=M=\dfrac{\sigma B_0^2}{\rho U_0}$,

Prandl Number $=P_r=\dfrac{\rho C_p\nu}{k}=\dfrac{\mu C_p}{k}$,

Eckert Number $=E_c=\dfrac{U_0^2}{C_p\left(T_w-T_\infty\right)}$,

Schmidt Number $=\mathcal{S}_c=\dfrac{\nu}{D}$,

Williamson Dimensionless Parameter $=\lambda=\dfrac{\Gamma}{\nu}\sqrt{\dfrac{U_0^3}{2x}}$

Chemical reaction parameter $R=-Rc\left(\dfrac{2x}{U_0}\right)$

Thermophoretic parameter $T_V=-\dfrac{k_T\left(T_W-T_\infty\right)}{T_\infty}$

The interesting physical parameters are the local skin-friction coefficient, the local Nusselt number, and the local Sherwood number which can be defined as follows [30]:

$$C_f=\frac{\tau_W}{\rho U_0^2},\ NU_x=\frac{xq_W}{k\left(T_W-T_\infty\right)},\ Sh_x=\frac{xq_M}{D\left(C_W-C_\infty\right)},$$

where $\tau_W=\mu\left[\dfrac{\partial u}{\partial y}+\dfrac{\Gamma}{\sqrt{2}}\left(\dfrac{\partial u}{\partial y}\right)^2\right]_{y=0}$, $q_W(x)=\left[-k\dfrac{\partial T}{\partial y}\right]_{y=0}$.

Using the similarity variable, we get:

$$\sqrt{2}C_f\mathrm{Re}_x^{1/2}=\left[f''(0)+\frac{\lambda}{2}\left(f''(0)\right)^2\right],\ NU_x\mathrm{Re}_x^{-1/2}=\frac{-\theta'(0)}{\sqrt{2}}$$

$$Sh_x\mathrm{Re}_x^{-1/2}=\frac{-\varphi'(0)}{\sqrt{2}}.$$

METHOD OF SOLUTION

The collection of non-linear partial differential equations Eqs. (2–4) were transformed into the ordinarily differentiable Eqs. (8–10) by using similarity transformation for the proposed parameter *Pr*, *M*, *Sc*, *Ec*, *λ*, *R*, *Tv*. Further, the equations Eqs. (8–10) are converted to first-order equations as follows:

$$f(1)=f,f(2)=f',f(3)=f'',f(4)=\theta,f(5)=\theta',$$
$$f(6)=\varphi,f(7)=\varphi',$$

and Eqs. (8–10), have been written as:

$$f'=\mathrm{f}(2)$$

$$f'''=\left(1/\left(1+\lambda*f(3)\right)\right)*\begin{pmatrix}\left(f(2)*f(2)\right)-\\ f(1)*f(3)\end{pmatrix}+M*f(2)$$

$$\theta'=\mathrm{f}(5)$$

$$\theta''=-\left(\mathrm{Pr}*f(1)*f(5)\right)-Ec*\mathrm{Pr}*f(3)*f(3)-M*\mathrm{Pr}*\mathrm{Ec}*f(2)*f(2)$$

$$\varphi'=\mathrm{f}(7)$$

$$\varphi''=-Sc*f(1)*f(7)-Sc*R*f(6)+\left(Tv*Sc*\begin{pmatrix}-\left(\mathrm{Pr}*f(1)*f(5)\right)\\ -Ec*\mathrm{Pr}*f(3)-\\ M*\mathrm{Pr}*\mathrm{Ec}*f(2)*f(2)\end{pmatrix}\right)$$

The bvp4c solver in MATLAB is employed to obtain numerical solutions for the above system. By analyzing graphical representations of fluctuations, we can investigate the influence of different parameters in the governing differential equations on the flow behavior. The problem involves essential dimensionless parameters like Prandtl number, Schmidt number, Eckert number, magnetic parameter, thermophoretic parameter, and chemical reaction parameter. A comprehensive examination of how various physical factors impact the velocity, concentration, and temperature of the fluid in close vicinity to the surface is obtained from these numerical solutions. The heat transfer parameter *-Θ'(0)* and mass transfer parameter -ϕ'*(0)* are also compared with [31] to evaluate the accuracy of our technique, and they agree very well with it. The association is provided in Table 1.

Table 1. Comparison value of -Θ'(0) and - ϕ'(0) for different Pr & Sc at λ= 0, R=0.0, M= 0, Ec = 0.

f(0)	Pr or Sc	[31] *-Θ'(0)* or -ϕ'*(0)*	Present Value *-Θ'(0)* or -ϕ'*(0)*
0	1	0.4439	0.4473
	10	1.680	1.6819
	100	5.545	5.5432

RESULTS AND DISCUSSION

The solution to the aforementioned problem is

illustrated by several graphs, each of which shows the outcomes for various parameter value sets. These values of the parameters set are taken from the earlier literature [4,5,32–35]. These graphs provide an extensive overview of the outcomes of computations. The relevant parameters including the Prandtl number, Schmidt number, Eckert number, magnetic parameter, thermophoretic parameter, and chemical reaction parameter are considered for the analysis.

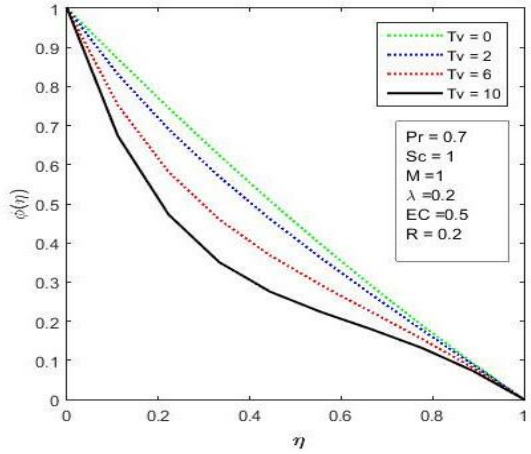

Figure 2. Concentration profile for different values of Tv.

Figure 2 highlights the effect of thermophoresis on the concentration profile. It has been noted that as the thermophoretic parameter increases, the thickness of the concentration at the boundary decreases. As the thermophoretic parameter increases, the thermophoretic force becomes stronger. Consequently, the fluid particles with higher concentration move towards regions of lower temperature, and those with lower concentration move towards regions of higher temperature. This migration of species leads to a reduction in the overall concentration profile. This behavior is clearly explained in Figure 2.

Figure 3 shows that the concentration profile is decreasing for an increasing value of the Schmidt number. When the Schmidt number increases, it implies that molecular diffusivity becomes less effective compared to momentum diffusivity. In other words, momentum transfer dominates over mass transfer. This has a significant impact on the concentration profile within the fluid. Consequently, the concentration gradients in the fluid become less pronounced, leading to a decreasing concentration profile.

Figure 4 shows that the concentration profile is decreasing for an increasing value of the chemical reaction parameter. As the chemical reaction rate increases, it leads to a faster conversion of the reactants into products. In a flow or medium, this results in a depletion of the species concentration as they are consumed more rapidly due to the increased chemical reaction rate. As a consequence, the overall concentration profile decreases along the flow direction.

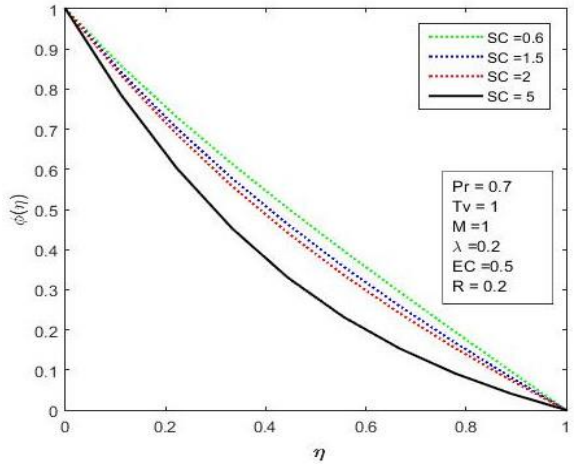

Figure 3. Concentration profile for different values of SC.

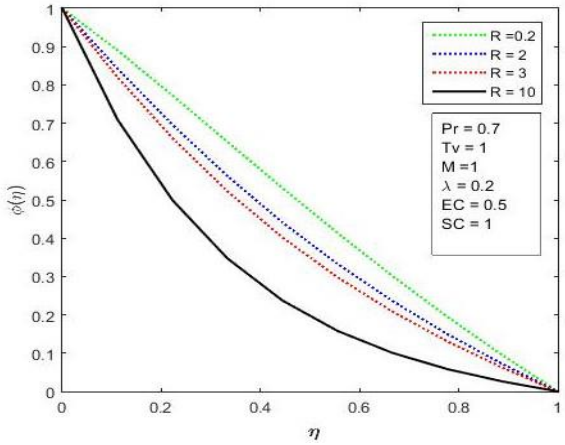

Figure 4. Concentration profile for different values of R.

From Figure 5, it is evident that the temperature profile increases as the Eckert number (Ec) increases. The increase of Eckert number indicates a greater kinetic energy relative to the enthalpy change, which can lead to enhanced convective heat transfer. This behavior is observed in Figure 5.

Figure 6 depicts the variations in temperature profiles for different parameter values Pr. When Pr is relatively low, thermal transmission becomes the dominant mode of heat transfer in the system. Consequently, heat can diffuse more quickly in such cases compared to scenarios where Pr has higher values. As a result, the temperature profile exhibits a steeper decline for smaller Pr values, indicating that heat dissipates more rapidly away from the heating surface. On the other hand, for higher Pr values, the dominance of thermal conduction diminishes, leading to slower heat diffusion and a less steep temperature decline. This behavior is clearly explained in Figure 6. Based on the findings presented in Figure 7, a

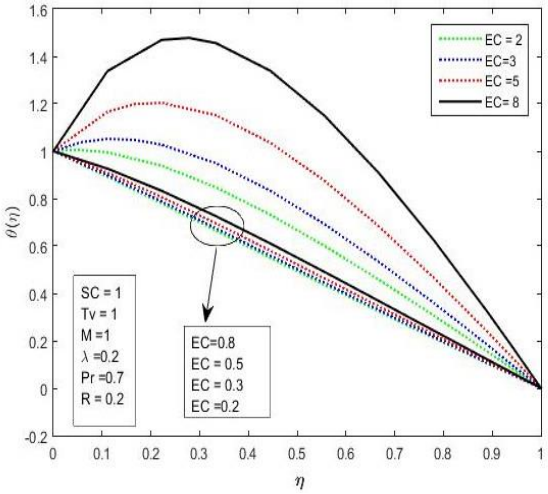

Figure 5. Temperature profile for different values of EC.

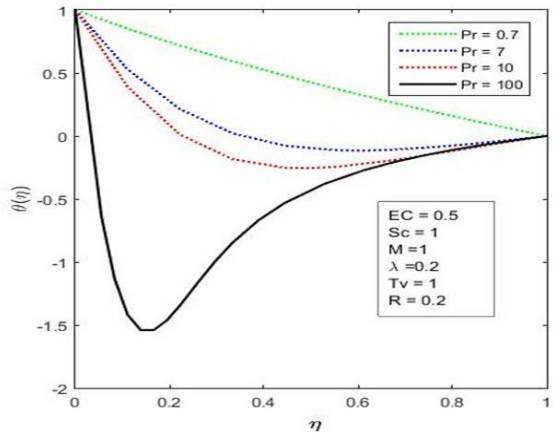

Figure 6. Temperature profile for different values of Pr.

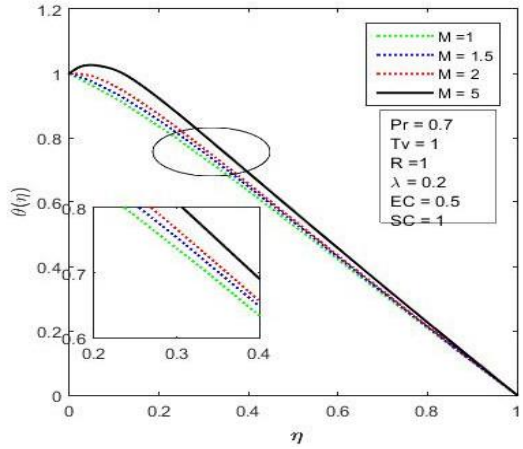

Figure 7. Temperature profile for different values of M.

noteworthy observation is that the temperature of the fluid rises with increasing values of the magnetic parameter (M). When M increases, it imposes a magnetic force on the fluid, which interacts with the fluid's motion and hinders its movement in turn it increases the temperature of the fluid. From Figure 8, it is observed that the velocity profile decreases for increasing Williamson dimensionless parameter.

From Figure 9, it is evident that as the magnetic parameter (M) increases, the fluid velocity progressively decreases. When M increases, it imposes a magnetic force on the fluid, which interacts with the fluid's motion and hinders its movement, thus impacting the velocity profile.

Figure 10 shows the variation in skin friction coefficient for various values of magnetic parameter (M). It is exhibited that the local skin friction coefficient has increased for a higher value of M. Heat transfer tendency of the fluid for different values of magnetic parameters (M) is shown in Figure 11. It is revealed that heat transfer is high for increasing magnetic parameters (M).

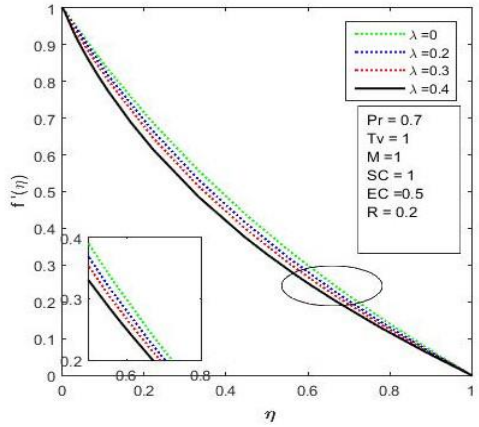

Figure 8. Velocity profile for different values of λ.

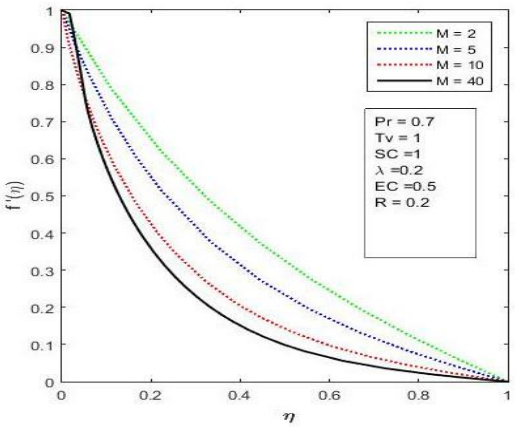

Figure 9. Velocity profile for different values of M.

The mass transfer tendency of the fluid for different values of the chemical reaction parameter (*R*) is shown in Figure 12. It is revealed that mass transfer is high for increasing chemical reaction parameter (*R*).

Future direction

In the literature survey, so far limited research has been made to analyze the problem of hybrid

nanoparticles with Williamson fluid model. Incorporating nanoparticles into Williamson fluid will enhance the traditional heat transfer properties because of their strong thermal conductivity. The idea of using Williamson nanofluid can be researched further in the future to enhance the heat transfer characteristics of the base fluid.

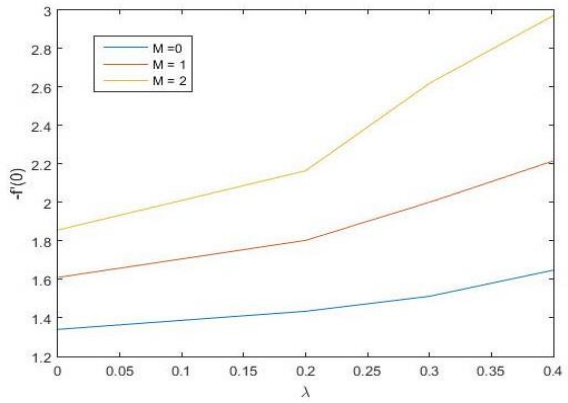

Figure 10. Skin friction coefficient for different value of M.

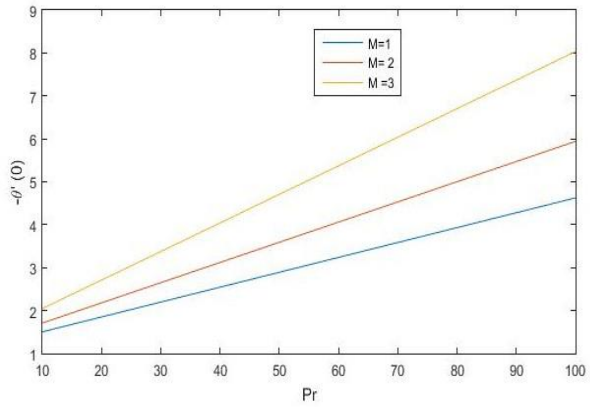

Figure 11. Heat transfer parameter for different values of of M.

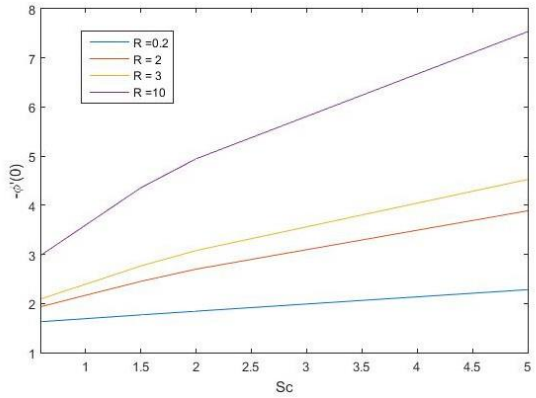

Figure 12. Mass transfer parameter for different values of of R.

CONCLUSION

The study focused on investigating the influences of various dimensionless factors on the temperature, velocity, and fluid concentration near the surface. The findings revealed significant trends in Williamson fluid, which are summarized as:

As the thermophoretic parameter increases, the strength of the thermal diffusion increases, which leads to the migration of species, and in turn, the concentration of the fluid decreases.

As Sc increases, the fluid's concentration near the surface diminishes.

As the chemical reaction factor rises, the fluid's concentration near the surface diminishes.

The fluid temperature rises with rising Eckert numbers suggesting higher Eckert numbers enhance heat transfer near the surface.

A rise in the Prandtl number causes the fluid temperature to rise suggesting that with lower values of Pr, thermal conduction is greater and that heat can diffuse and move away from the heat surface more quickly than at higher values of Pr.

The increase in the magnetic parameter (M) leads to an increase in the fluid temperature distribution and causes a decrease in the velocity profile.

The velocity profile diminishes as the Williamson dimensionless parameter increases.

Nusselt number and skin friction coefficient increase with increasing magnetic parameters, and Sc increases with increasing chemical reaction parameters.

NOMENCLATURE

U_0 stretching parameter
Ec Eckert number
Sc Schmidt number
Cp specific heat at constant pressure
C fluid concentration
T fluid temperature
Pr Prandtl number
B Magnetic field
M magnetic parameter

Greek symbols

η similarity variable
ϕ dimensionless concentration
λ Williamson fluid parameter
μ dynamic viscosity
ν kinematic viscosity
ρ density of the fluid
σ electrical conductivity
Ψ stream function
θ dimensionless temperature
k thermal conductivity

Subscripts

w conditions at the surface
∞ conditions far away from the surface

REFERENCES

[1] R.V. Williamson, Ind. Eng. Chem. Res. 21(1929) 1108–1111. https://doi.org/10.1021/ie50239a035.

[2] B.C. Sakiadis, AIChe J. 7 (1961) 26–28. https://doi.org/10.1002/aic.690070108.

[3] F.K. Tsou, E.M. Sparrow, R.J. Goldstein, Int. J. Heat Mass Transfer 10 (1967) 219–235. https://doi.org/10.1016/0017-9310(67)90100-7.

[4] L.E. Erickson, L.T. Fan., V.G. Fox, Ind. Eng. Chem. 5 (1966) 19–25. https://doi.org/10.1021/i160017a004.

[5] S. Nadeem, S.T. Hussain, C. LeeBraz. J. Chem. Eng. 30(3) (2013) 619–625. https://doi.org/10.1590/S0104-66322013000300019.

[6] T. Hayat, A. Shafiq, A. Alsaedi, Alexandria Eng. J. 55(3) (2016) 2229–2240. https://doi.org/10.1016/j.aej.2016.06.004.

[7] H.M. Shawky, N.T. Eldabe, K.A. Kamel, E.A. Abd-Aziz, Microsyst. Technol. 25(4) (2018) 1155–1169. https://doi.org/10.1007/s00542-018-4081-1.

[8] S. Nadeem, S.T. Hussain, Appl. Nanosci. 4(8) (2014) 1005–1012. https://doi.org/10.1007/s13204-013-0282-1.

[9] S. Nadeem, S.T. Hussain, J. Appl. Fluid Mech. 9 (2) (2016) 729–739. https://doi.org/10.18869/acadpub.jafm.68.225.21487.

[10] T. Kebede, E. Haile, G. Awgichew, T. Waleign, J. Appl. Math. 2020 (2020) 1–13. https://doi.org/10.1155/2020/1890972.

[11] I.C. Liu, Int. Commun. Heat Mass Transfer 32 (8) (2005) 1075–1084. https://doi.org/10.1016/j.icheatmasstransfer.2005.02.003.

[12] M.A.A. Hammad, M. Ferdows, Appl. Math. Mech. 33 (7) (2012) 923–930. https://doi.org/10.1007/s10483-012-1595-7.

[13] F.M. Ali, R. Nazar, N.M. Arifin, I. Pop, Appl. Math. Mech. 32 (4) (2011) 409–418. https://doi.org/10.1007/s10483-011-1426-6.

[14] V. Kumaran, G. Ramanaiah, Acta Mech. 116 (1–4) (1996) 229–233. https://doi.org/10.1007/BF01171433.

[15] M.E. Ali, Int. J. Heat Mass Transfer 16 (1995) 280–290. https://doi.org/10.1016/0142-727X(95)00001-7.

[16] E.M.A. Elbashbeshy, Arch. Mech. 53 (6) (2001) 643–651. https://am.ippt.pan.pl/am/article/viewFile/v53p643/pdf.

[17] E. Sanjayanand, S.K. Khan, Int. J. Therm. Sci. 45 (2006) 819–828. https://doi.org/10.1016/j.ijthermalsci.2005.11.002.

[18] E. Magyari, B. Keller, J. Phys. D: Appl. Phys. 32 (1999) 577–585. http://doi.org/10.1007/s002310000126.

[19] S. Nadeem, S. Zaheer, T. Fang, Numer. Algorithms 57 (2011) 187–205. http://dx.doi.org/10.1007/s11075-010-9423-8.

[20] E.Sanjayanand, S. K. Khan, Intl. J. Therm. Sci. 45, (2006) 819–828. https://doi.org/10.1016/j.ijthermalsci.2005.11.002.

[21] E. Magyari, and B. Keller, J. Physics D: Appl. Physics, 32, (1999) 577–585. http://dx.doi.org/10.1088/0022-3727/32/5/012.

[22] S. Nadeem, S. Zaheer, T. Fang, Numer. Algorithms 57, (2011) 187–205. http://dx.doi.org/10.1007/s11075-010-9423-8.

[23] S. Nadeem, C. Lee, Nanoscale Res. Lett. 7, (2012) 94 https://doi.org/10.1186/1556-276X-7-94.

[24] M.S. Arif, K. Abodayeh, Y. Nawaz, Axioms,12(5), (2023) 460, https://doi.org/10.3390/axioms12050460.

[25] Y. Nawaz, M.S. Arif, K. Abodayeh, Int. J. Numer. Methods Fluids, 94 (7), (2022) 920–940. https://doi.org/10.1002/fld.5078.

[26] P. Loganathan, N.G. Stepha, J. Appl. Fluid Mech, 6(4), (2013) 581–588. 10.36884/JAFM.6.04.21276.

[27] M. Ismail, D.M. Gururaj, Heat Transf. 50(4) (2021), 4019–4038 https://doi.org/10.1002/htj.22062.

[28] M. Ismail, D.M. Gururaj, J. Nanofluids, 12 (3), (2023), 809–818. https://doi.org/10.1166/jon.2023.1962.

[29] M. Ismail, D.M. Gururaj, Numer. Heat Transf. B: Fundam. (2023) 1–27. https://doi.org/10.1080/10407790.2023.2257381.

[30] P. Loganathan, N. Golden Stepha, Asia Pac. J. Chem. Eng. 8(6) (2013), 870–879 https://doi.org/10.1002/apj.1732.

[31] L.E. Erickson, L.T Fan, V.G. Fox, Ind. Eng. Chem. Fundam. 5(1), (1966), 19–25. https://doi.org/10.1021/i160017a004.

[32] V.K. Garg, S. Jayaraj. Int. J. Heat Mass Transfer, 31 (1998) 875–890. https://doi.org/10.1016/0017-9310(88)90144-5.

[33] N.A. Khan, H. Khan, Nonlinear Eng. 3(2), (2014)107–115. https://doi.org/10.1515/nleng-2014-0002.

[34] H. Maaitah, A.N. Olimat, O. Quran, H.M. Duwairi, Int. J. Thermofluids, 19 (2023) 100361. https://doi.org/10.1016/j.ijft.2023.100361.

[35] A.M. Megahed, IJMPC, 31(1), (2020) 2050019. http://doi.org/10.1142/S0129183120500199.

GOLDEN STEPHA NALLATHAMBI[1]

BHARATHI GOWRI SASI KUMAR[2]

GUVVA SWATHY[3]

[1]Department of Mathematics, R.M.K Engineering College, India

[2]Department of Mathematics, Ethiraj College for Women, India

[3]Mathematics Department, S. A. Engineering College, India

NAUČNI RAD

MAGNETOHIDRODINAMIČKI VILIJAMSONOV TOK TEČNOSTI NA PRODUŽENOJ PLOČI SA TERMOFOREZOM I HEMIJSKOM REAKCIJOM

U ovom radu je istraživan stabilan, dvodimenzionalni, nestišljiv tok pseudoplastične Vilijamsonove tečnosti podvrgnute linearno rastegnutom sloju. Studija uključuje efekte magnetnih polja, hemijskih reakcija i termoforeze na ponašanje fluida. Primenom metoda graničnog sloja i sličnosti, glavne jednačine su pojednostavljene za numeričku analizu. Za rešavanje redukovanih jednačina koristi se MATLAB bvp4c rešavač. Dobijeni rezultati su vizuelno predstavljeni i detaljno razmotreni kako bi se sagledale fizičke karakteristike modela. Istraživanje naglašava uticaj magnetnog polja, hemijske reakcije i uticaj taloženja čestica termoforezom na strujno ponašanje Vilijamsonove tečnosti preko produžene ploče. Značajne uloge u određivanju koncentracije tečnosti u blizini graničnog sloja imaju hemijske reakcije i parametri termoforeze. Primećeno je da povećanje parametara hemijskih reakcija i termoforeze dovodi do smanjenja debljine koncentracije tečnosti u blizini graničnog sloja. Primetno je da je povećanje Šmitove vrednosti takođe smanjilo debljinu koncentracije tečnosti blizu graničnog sloja. Magnetohidrodinamički parametar značajno utiče na brzinu tečnosti i temperaturu blizu površine. Primećeno je da povećanje magnetohidrodinamičkog parametra smanjuje brzinu fluida i povećava temperaturu blizu površine. Razmatraće se uticaji koeficijenta trenja, Nuseltovog broja i koeficijenta prenosa mase na Vilijamsonovu tečnost. Dobijeni nalazi se porede sa postojećim istraživanjima, a korelacija je data tabelarno.

Ključne reči: Vilijamsonov fluid, magnetohidrodinamika, hemijska reakcija, termoforeza.